URSI GASS 2021, Rome, Italy, 28 August - 4 September 2021

A statistical approach towards the equivalence of HIRF and DCI test setups

Jan Ückerseifer*, Tianyuan Kong, and Frank Gronwald
Institute for Reliability of Technical Systems and Electrical Measurement, University of Siegen, Hölderlinstr. 3, 57076 Siegen, Germany

Abstract

This contribution analyzes the equivalence of radiated and conducted EMC tests on a statistical basis. Via numerical simulations of HIRF and DCI setups using a simplified vehicle as test object, the statistical properties of the electric field within this vehicle are compared. It turns out that the modulus of each cartesian electric field component for both HIRF and DCI can be characterized by Rayleigh distributions with similar parameters. Consequently, from a statistical point of view, HIRF and DCI tests can generate comparable field distributions.

1 Introduction

Immunity testing in EMC can be either performed by radiated or conducted excitations. A very well established procedure standardized in [1] is known as HIRF (High Intensity Radiated Field), which exposes a DUT (Device Under Test) to a defined field strength, test frequency, polarization and illumination angle with the help of a transmitting antenna.
A conducted counterpart to HIRF mainly used in avionics is the procedure of DCI (Direct Current Injection) specified in [2]. Here, surface currents are injected to a DUT via current sources galvanically connected to the DUT. In this manner, DCI seeks to approximate the surface currents on DUTs generated during HIRF tests via induction.
A problem with regard to DCI is its restricted usability for high test frequencies. Usually, only the lowest resonances of a DUT can be tested, which could be shown for a generic test object in [3]. Especially if geometrically more complex test objects are considered, the frequency range of DCI is limited, see [4]. In contrast, HIRF is suitable at high test frequencies, but difficult to realize for low test frequencies, as the field homogeneity deteriorates. Besides, increasing antenna dimensions and the need for performant power amplifiers imply economic drawbacks.
For intermediate frequencies both HIRF and DCI are applicable, such that equivalence considerations of both approaches are of interest. The correlation of both HIRF and DCI was subject to several investigations, such as [3], [5], [6]. A non-statistical approach was used in [7] by comparing the surface currents on the metallic surface of generic DUTs with the help of Characteristic Mode Analysis.
Instead of illuminating a DUT directly, like in HIRF testing, the DUT can alternatively be illuminated within a reverberation chamber. Generally, reverberation chambers are only applicable at high test frequencies but already have been investigated in combination with DCI as well [8]. Due to the various reflections, the electric field is not deterministic anymore, but can instead be described by probability density functions. It could be furthermore shown in [9] that the same probability densities not only hold for reverberation chambers, but also for DUTs, whose interior dimensions are electrically large, like road vehicles.
This observation can be exploited to compare EMC testing with HIRF and DCI, because if both procedures show the same field distributions and their probality densities have similar parameters, HIRF and DCI can be regarded as equivalent from a statistical point of view. This issue is investigated in the following for different HIRF and DCI scenarios using a generic vehicle model as DUT.

2 Statistical theory of reverberation chambers

The field distribution of the electric field in reverberation chambers has been analyzed in numerous publications like [10], [11], [12].
Let E_x, E_y, E_z denote scalar cartesian components of the electric field, where each component consists of a real and an imaginary part, e. g. $E_x = |\underline{E}_x| = |E_{x,r} + \mathrm{j}E_{x,i}|$ for the x-component. Then, all real and imaginary parts are known to obey a normal distribution.
Furthermore, the moduli E_x, E_y, E_z of single cartesian field components follow a Rayleigh distribution, described by the probability density

$$P(X = x) = \frac{x}{\sigma^2} \exp\left(-\frac{x^2}{2\sigma^2}\right) \tag{1}$$

with σ as a distribution's characteristic parameter and X as random variable equalling the electric field. A Rayleigh distribution is a special case of a χ-distribution, more precisely a χ_2-distribution. The total electric field $E_{\mathrm{tot}} = \sqrt{E_x^2 + E_y^2 + E_z^2}$, eventually, is χ_6- distributed.
The aforementioned relations only hold for measurements

in a sufficiently large distance from the vehicle's conducting walls, since the tangential components of the electric field vanish on these boundaries, leading to less degrees of freedom [13].

3 Numerical Setups

The HIRF and DCI excitations to compare are simulated in CST Microwave Studio [14]. Figure 1 illustrates a simplified vehicle modeled as rectangular box with dimensions 1580 x 1530 x 3540 mm serving as test object [9]. It contains apertures comparable to windows in a real passenger vehicle, through which the field can penetrate. The perfectly conducting vehicle is positioned 300 mm above a ground plane and the background is modeled as free space.

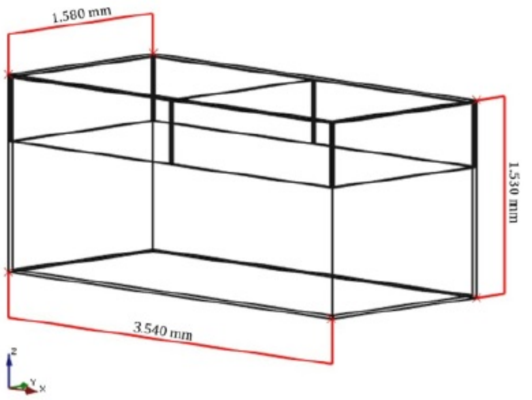

Figure 1. HIRF setup

A vertically polarized plane wave with 224 MHz and 1V/m is used as excitation source and the excitation plane has a distance of 500 mm to the vehicle.
Within the vehicle, 420 equidistantly spaced electric field probes with a 200-mm exclusion zone to the walls are placed, see Figure 2. From the measured field data, histograms for the electric field can be created, from which the field distributions are deduced as probability densities.

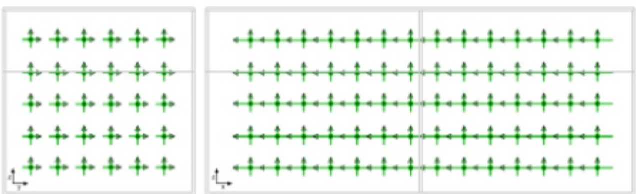

Figure 2. Electric field probes inside the vehicle (left: front view, right: top view)

Regarding the HIRF simulations, three different illumination directions are investigated. They are indicated in Figure 3 by means of the plane wave's propagation vector β with indices {1,2,3} identifying each scenario. The first illumination exposes the vehicle's front, the second one its side and the third one its front edge.

The DCI setup modeled in CST is depicted in Figure 4. It is

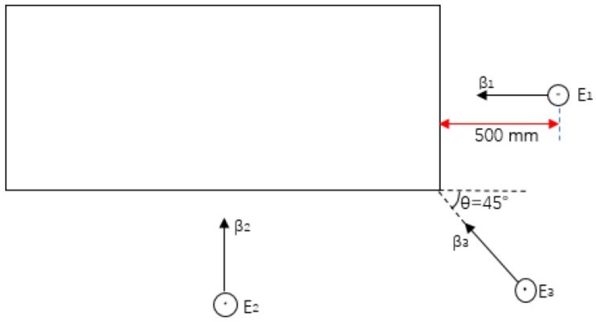

Figure 3. Excitation scenarios for HIRF testing (top view)

excited via current sources with an impedance of 50 Ω and terminated by a discrete 50 Ω resistor. Similar to the HIRF configuration, three different excitation scenarios are considered. In order to approximate the illumination directions of HIRF, three current sources are connected to the vehicle's front, side and edge. For this purpose, two metallic boundaries perpendicular to the ground plane were added in CST. Note that only one current source per simulation is active.

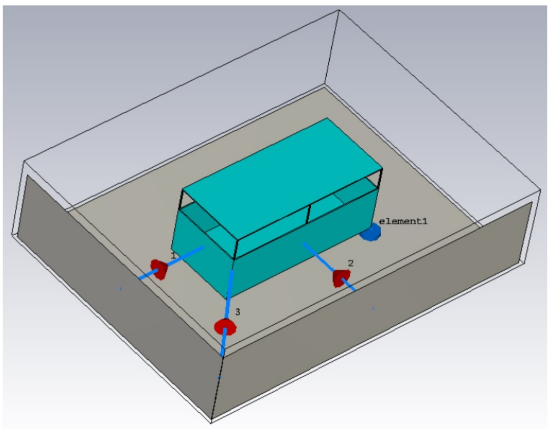

Figure 4. DCI setup with three current sources

4 Results

The electric fields retrieved from the field probes are separated into classes, each representing a specific amplitude range, such that a histogram is deducable. In order to determine the corresponding probability density, a distribution fitter implemented in MATLAB [15] is applied. It is capable of fitting probability densities to the electric field data and additionally calculates the characteristic parameters of these distributions.
According to the fitter's analysis, assuming a HIRF excitation of the vehicle's front, the electric field inside the vehicle for all cartesian components is Rayleigh-distributed, see Figure 5. It is observable that higher field strengths compared to the excitation amplitude of 1 V/m are measured as a consequence of multiple reflections and superpositions, especially for the E_z-component. For E_x and E_y the most probable field strength approximately equals the excitation

amplitude. The density functions for all excitation scenarios of Figure 3 are defined by the parameter σ in Table 1 for each cartesian component.

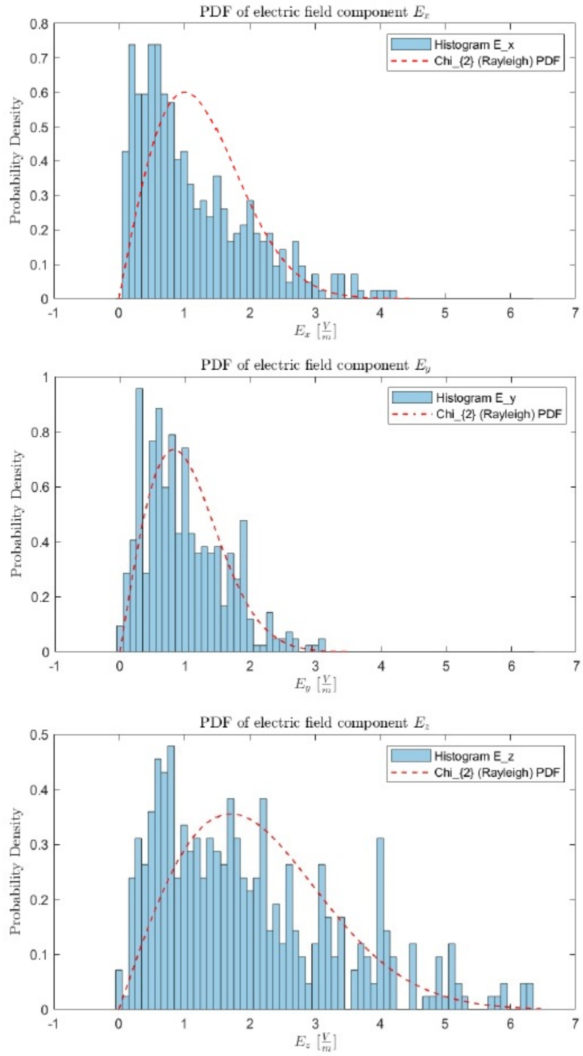

Figure 5. Histograms and probability densities for E_x, E_y, E_z assuming HIRF testing

Table 1. Parameter σ for the three HIRF setups

Scenario	σ_x	σ_y	σ_z
1	1.0111	0.8255	1.707
2	1.0529	0.8143	0.7616
3	1.0805	0.6267	1.3593

Computing the statistical behavior for a DCI excitation of the vehicle's front leads to the histograms and fitted density functions in Figure 6, in which the corresponding densities of Figure 5 are inserted in black for better comparison. As determined by MATLAB, the electric field is best fitted by a Rayleigh distribution, just like for the HIRF setup. A comparison to the HIRF results reveals, that both test procedures evoke similar field distributions. The most probable field strength of both procedures only differs about 0,2 V/m from each other.

Nevertheless, there remain certain deviations, which can be also seen in Table 2 listing the σ values for all three excitation scenarios of Figure 4. This is explainable by the different wave propagation in HIRF and DCI testing. Whereas the plane wave irradiates the vehicle's apertures directly, the DCI current basically propagates along the vehicle's bottom part.

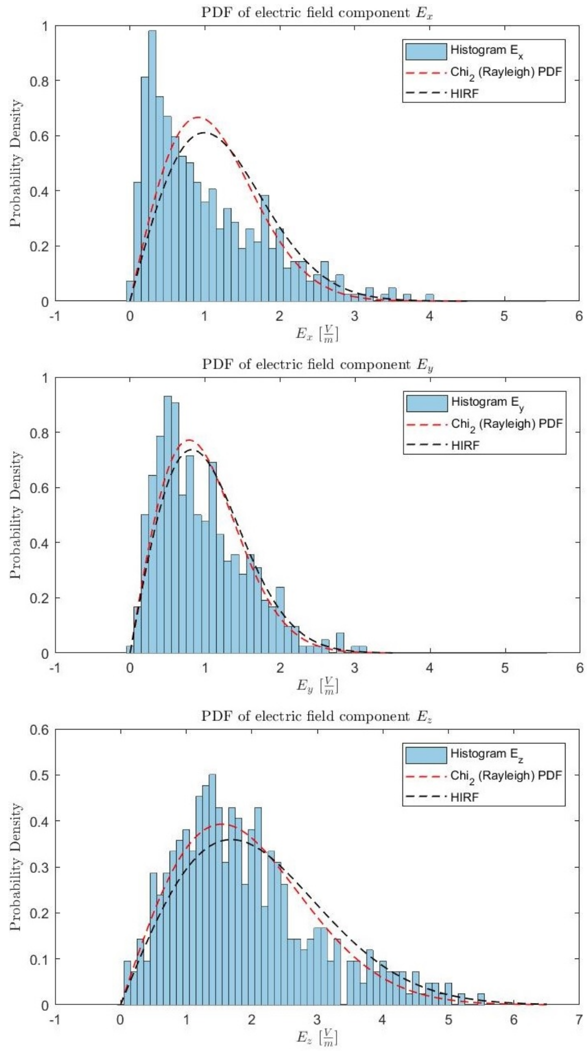

Figure 6. Histograms and probability densities for E_x, E_y, E_z assuming DCI testing

Table 2. Parameter σ for the three DCI setups

Scenario	σ_x	σ_y	σ_z
1	0.9105	0.7861	1.5438
2	1.2817	0.9567	1.9670
3	0.8823	0.6961	0.9310

In addition to the presented results at a test frequency of 224 MHz, field simulations for HIRF and DCI at higher frequencies up to 1 GHz were carried out. In particular, an improved field homogeneity could be observed here, since the mode density inside the vehicle is significantly increased [16]. Due to the limited extent of this paper, these results cannot be presented in detail.

5 Conclusion

HIRF as well as DCI excitations were examined with focus on their impact on field distributions inside reverberating systems. For the HIRF setup, the common statistical behavior for the electric field inside reverberation chambers described in literature could be reproduced. All cartesian field components were found to be Rayleigh-distributed, no matter which illumination scenario is chosen.
Concerning the DCI excitations, a similar statistical field distribution is accomplished. The field components inside the vehicle likewise obey Rayleigh distributions with similar parameters. It can thus be assumed that the kind of excitation is not primarily responsible for the field distribution, but the reverberating system itself along with its resonance characteristics. The probability densities for HIRF and DCI are in overall good agreement, yet some deviations caused by the physically different test setups can be recognized.

6 Acknowledgements

The authors thank Martin Aidam and Markus Rothenhäusler for important discussions. This research was supported by the Federal Ministry of Transport and Digital Infrastructure of Germany, BMVI, in the funding program Automated and connected driving, LINKTEST (grant no. 16AVF2138A)

References

[1] ISO 11451-2, “Road vehicles - Vehicle test methods for electrical disturbances by narrowband radiated electromagnetic energy - Part 2: Off vehicle radiation source”, International Organization for Standardization, 1999.

[2] ED-107A, “Guide to Certification of Aircraft in a High Intensity Radiated Field (HIRF) Environment”, European Organization for Civil Aviation Electronics, 2015.

[3] M. Rothenhäusler, A. Ruhfass and T. Leibl, “Broadband DCI as a multi usable EMC-test method”, 2008 IEEE International Symposium on Electromagnetic Compatibility, Detroit, MI, 2008, pp. 1-5, doi: 10.1109/ISEMC.2008.4652003.

[4] J. Ückerseifer and F. Gronwald, “Numerical and Experimental Analysis of Non-Coaxial DCI-Excitations as HIRF-Replacement in Automotive Immunity Testing”, 2020 International Symposium on Electromagnetic Compatibility, Rome, Italy, 2020, pp. 1-6, doi: 10.1109/EMCEUROPE48519.2020.9245717.

[5] G. A. Rasek and S. E. Loos, “Correlation of Direct Current Injection (DCI) and Free-Field Illumination for HIRF Certification”, in IEEE Transactions on Electromagnetic Compatibility, vol. 50, no. 3, pp. 499-503, Aug. 2008, doi: 10.1109/TEMC.2008.926872.

[6] A. M. Wellington, “Direct current injection as a method of simulating high intensity radiated fields (HIRF)”, IEE Colloquium on EMC Testing for Conducted Mechanisms, London, UK, 1996, pp. 4/1-4/6, doi: 10.1049/ic:19960731.

[7] J. Ückerseifer, M. Aidam, M. Rothenhäusler and F. Gronwald, “A Numerical Analysis of HIRF- and DCI-Equivalence by Characteristic Mode Theory”, 2019 International Symposium on Electromagnetic Compatibility, Barcelona, Spain, 2019, pp. 315-320, doi: 10.1109/EMCEurope.2019.8871548.

[8] M. Rothenhäusler, A. Schoisl and M. Schwarz, “Numerical Simulation of a Direct Current Mode Stirred Reverberation Chamber”, 2019 International Symposium on Electromagnetic Compatibility - EMC EUROPE, Barcelona, Spain, 2019, pp. 247-252, doi: 10.1109/EMCEurope.2019.8872037.

[9] T. Konefal, A. C. Marvin, J. F. Dawson and M. P. Robinson, “A Statistical Model to Estimate an Upper Bound on the Probability of Failure of a System Installed on an Irradiated Vehicle”, in IEEE Transactions on Electromagnetic Compatibility, vol. 49, no. 4, pp. 840-848, Nov. 2007, doi: 10.1109/TEMC.2007.908265.

[10] David A. Hill, “Electromagnetic Theory of Reverberation Chambers”, Nat. Inst. Standards Technol., Technol. Admin., U.S. Dept. Comm., Helena, MT, Tech. Note 1506, Dec. 1998.

[11] M. P. Robinson, J. Clegg and A. C. Marvin, “Radio frequency electromagnetic fields in large conducting enclosures: effects of apertures and human bodies on propagation and field-statistics”, in IEEE Transactions on Electromagnetic Compatibility, vol. 48, no. 2, pp. 304-310, May 2006, doi: 10.1109/TEMC.2006.873856.

[12] T. Panaretos, C. A. Balanis and C. R. Birtcher, “HIRF penetration into simplified fuselage using a reverberation chamber approach”, in IEEE Transactions on Electromagnetic Compatibility, vol. 47, no. 3, pp. 667-670, Aug. 2005, doi: 10.1109/TEMC.2005.851729.

[13] J. G. Kostas and B. Boverie, “Statistical model for a mode-stirred chamber”, in IEEE Transactions on Electromagnetic Compatibility, vol. 33, no. 4, pp. 366-370, Nov. 1991, doi: 10.1109/15.99120.

[14] Dassault Systemes, CST Studio Suite 2018, Version 2018.06.

[15] MathWorks, MATLAB, Version R2017b.

[16] B.-H. Liu, D. Chang, M. Ma, “Eigenmodes and the composite quality factor of a reverberating chamber”, National Bureau of Standards, NBS. August 1983 (TN 1066). - NBS Technical Note. - 1-46 S.